

Distribution of stresses along the length of BFRP rods glued-in to Irish Sitka Spruce

Caoimhe O'Neill¹, Daniel McPolin¹, Su Taylor¹, Annette Harte²

¹School of Planning, Architecture and Civil Engineering, David Keir Building, Queen's University Belfast, Belfast, Co. Antrim, Northern Ireland, BT9 5AG

²College of Engineering and Informatics, Engineering Building, National University of Ireland, Galway, University Road, Galway, Co. Galway, Ireland.

email: coneill86@qub.ac.uk, d.mcpolin@qub.ac.uk, s.e.taylor@qub.ac.uk, annette.harte@nuigalway.ie

ABSTRACT: Glued-in rods (GiR) present a viable alternative to traditional steel moment connections in both new build and retrofit of timber structures. Limited research has been carried out on the distribution of stresses along the glued length of a rod under a load combination of axial force and bending moment. Previous research has found that under an axial-only load with short embedded lengths the entire length of the rod reaches peak stress at once and fails at a relatively low load with high peak stress. At longer embedded lengths failure is more gradual, with one end reaching peak stress before the other leading to a higher failure load and lower peak stress. This research aims to confirm that this holds for combined loading also; that stresses are not distributed evenly along the embedded length of a GiR and that failure arises at the loaded end due to a peak in stress concentration at this location. Electrical Resisting Strain gauges and Draw Tower Grating fibre optic sensors were used to capture the stress profile along the length of the GiR. Embedded length and edge distance were varied to investigate the effect of these variables on stress distribution. Specimens were tested under a pull-bending test set-up. Generally, a linear increase in strain was observed at each measured location until failure. In all specimens, failure was observed to occur with a stress peak towards the loaded end. In a number of specimens peak stress was observed to move away from the loaded end as the specimen approached failure, suggesting the bond at this end had failed.

KEY WORDS: Glued-in rods; Timber; Stress distribution; Composites.

1 INTRODUCTION

The development of lightweight, corrosion resistant and sustainable moment resistant timber connections using glued-in rods (GiR) would facilitate the adoption of timber elements in large construction projects.

Glued-in rods present a sustainable, aesthetically pleasing alternative to the cumbersome conventional steel moment connections that are often encountered in timber construction. Not only do connections with glued-in rods look better than conventional connections, they also have enhanced fire protection as the rods which transfer moment are embedded inside, and are therefore protected by, the timber.

Glued-in rods have significant potential in a wide range of both new build and restoration projects. Successful renovation has been carried out in roof and floor beams in buildings subject to decay [1], [2]. In new build, five areas were identified where glued-in rods may be used for connections: frame corner, beam-post connection, beam-beam joint, supports and hinged joints [3].

Since the late 1980s there have been many research projects commissioned on the use of bonded-in rods in timber construction e.g. GIROD and LICONS [4], [5]. In spite of this, no universal standard exists for their design. There had been an informative annex in the pre-standard PrBS ENV 1995-2:1997 which provided limited coverage of the design of bonded-in rods using steel bars however this document was replaced by BS EN 1995-2:2004 and no guidance is included in this current document.

While GiR are often steel some other rod types have been studied, namely Fibre Reinforced Polymers (FRPs). Earlier studies investigated the use of glass fibre reinforced polymer (GFRP) as an alternative to steel [6]–[8] while carbon fibre reinforced polymer (CFRP) has been used more recently [9]. Despite its significant cost effectiveness compared to CFRP and its greater tensile strength compared to GFRP, basalt fibre reinforced polymer (BFRP) has only been investigated in a very limited manner for use in glued-in technology [10]. BFRP has a modulus of elasticity closer to timber than the more commonly used material, steel. It is also a much lower cost material compared to the other FRPs. These advantages resulted in the selection of BFRP for use in this research.

The stress distribution along a GiR is generally considered to show a peak at the loaded end with dissipation of the stress occurring along the length of the rod as suggested by [11], [12] for axially loaded systems. At a fixed loading rate it appears that for short embedded lengths almost the entire length of the rod reaches peak stress at once and hence fails at a relatively low load and with high peak stress. At longer embedded lengths failure is more gradual, with one end reaching peak stress before the other leading to a higher failure load and lower peak stress.

Other research found that long embedded lengths resulted in minimal change in stress concentrations beyond the optimum embedded length and thus suggest that the bondline becomes inactive beyond the optimum length [13].

This research aims to determine if this assumption of stress distribution is valid for pull-bending mechanisms where the glued-in rod is under a combination loading; that stresses are not distributed evenly along the embedded length of a GiR and that failure arises at the loaded end due to a peak in stress concentration at this location.

2 TEST PROCEDURE

2.1 Background

Embedded length is one of the most influential variables on the strength of glued-in rods. A preliminary study was performed to assess how embedded length affected the pull-out strength of glued-in BFRP rods in Irish Sitka Spruce. As was anticipated, an increase in pull-out strength was observed with an increase in embedded length. It was observed that between the shortest embedded length of 80mm and the longest length of 600mm the pull-out capacity increased by a factor of 2.13. This was as expected since the larger interface area with each increase in embedded length provides additional resistance to the applied loading. Optimum embedded length was identified as $l_b=280\text{mm}$. At this point sufficient pull-out strength was achieved to resist loading that would be experienced in service.

Splitting was observed in several of the specimens of optimum embedded length. In these specimens failure strength was significantly lower than in specimens where no splitting was observed. In an attempt to alleviate this problem, a set of specimens were tested where embedded length remained at 280mm but edge distance increased in steps of one bar diameter. It was found that by increasing the edge distance by even a small amount instances of splitting could be reduced or eliminated, thus allowing specimens to reach their full potential capacity. The optimum edge distance was identified as $a=42\text{mm}$. This edge distance provided a good balance between a significant reduction in instances of splitting and a large enough lever arm to generate bending moment in the system.

2.2 Materials

Class C16 Irish Sitka Spruce (*Picea sitchensis*), sourced from Balcas Sawmill in Northern Ireland with a size of 75mm x 225mm sawn section was used. Material testing revealed that this timber had a 5th percentile bending strength $f_{m,k}=16.8\text{N/mm}^2$, shear strength $f_{v,k}=8.7\text{N/mm}^2$ and a density $\rho_k=381\text{kg/m}^3$.

Basalt Fibre Reinforced Polymer (BFRP) rods of 12mm diameter were used in this experimental programme. These rods were found to have a tensile strength of 920N/mm^2 under a low loading rate of 0.2kN/s [14]. Unlike steel or some other FRPs, no extensive cleaning of the rods was required prior to bonding as they are sand-coated which provides a good surface for adhesion.

In a number of studies it was determined that epoxy adhesives had higher strength than phenol resorcinol or polyurethane alternatives and that epoxies are most suitable for glued-in rod applications [15], [16]. A two-part thixotropic gap filling epoxy was used to ensure the bond had a higher shear strength

and stiffness than the timber being used. This adhesive only flows under shear so is ideal for GiR applications such as overhead beam repair or jointing overhead. The Rotafix epoxy used is comprised of a base which is an epoxy resin and a polyetheramine mixture hardener. The epoxy had a bond strength of $6\text{-}10\text{N/mm}^2$ after curing for a minimum of five days [17].

2.3 Test set-up

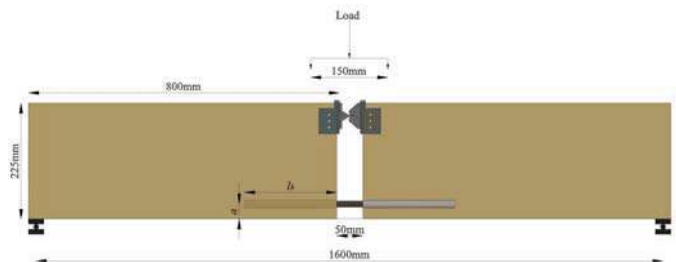


Figure 1. Configuration of Pull-bending test

Pull-out capacity can be used as a measure of the strength of a glued-in rod. The pull-out test system used was a pull-bending set-up, as pictured in Figure 1. The pull-bending system allows bending strength of the glued-in rod connection to be evaluated by removing the timber in the section being loaded so that the only resistance is from the BFRP bars glued-in to the timber.



Figure 2. a) ERS gauge, b) DTG fibre mounted on BFRP rod

Two methods were used to obtain the stress profile along the length of the GiR: Electrical Resisting Strain (ERS) gauges and Draw Tower Grating (DTG) fibre optic sensors. The sensors were attached directly on to the BFRP rod as per Figure 2 to assess the how stresses were distributed along the glued length under loading.

Electrical resisting strain (ERS) gauges relate small changes in length to a change in current, allowing measurement of microstrain. 30mm gauges were used. A noted disadvantage of their use is that they are relatively large and require wiring which may interfere with the bond in a GiR. DTG measure strain by detecting a change in wavelength of light reflected along a fibre optic sensor. This change in wavelength correlates to a change in strain. In the manufacture of DTGs the fibre is notched whilst being pulled resulting in a more

mechanically stable fibre than traditional fibre Bragg gratings. The fibre is reasonably simple to install as it is glued on to the sanded surface of the rod with a fast setting adhesive. The fibre is however relatively fragile therefore care must be taken during installation not to catch the fibre on a sharp edge or to bend the fibre excessively. Testing is slower when using DTGs as they measure strain within a fixed wavelength range. If the range is exceeded the test must be paused to allow recalibration of the wavelength range.

Stress distribution was assessed in a number of specimens to monitor how distribution changed with varying edge distance and with varying embedded length. For these tests optimum embedded length and edge distance had been identified through earlier testing.

A number of configurations were analysed using both strain acquisition methods. This allowed a comparison between both methods of measurement. The composition of the sample set is given in Table 1.

Table 1. Configuration of test specimens

	ID	l_b (mm)	a (mm)	Location of readings (mm from loaded end)
Edge Distance	ERS1	280	42	0, 70, 140, 210, 280
	ERS2	280	54	0, 70, 140, 210, 280
	ERS3	280	66	0, 70, 140, 210, 280
Embedded Length	ERS4	80	42	0, 20, 40, 60, 80
	ERS5	600	42	0, 150, 300, 450, 600
	DTG1	80	42	0, 20, 40, 60, 80
	DTG2	280	42	0, 20, 70, 140, 210, 280
	DTG3	600	42	0, 20, 150, 300, 450, 600

2.4 Specimen fabrication

Rods were cut to length and sanded local to the position of the ERS gauges. The gauges were then glued directly on to the rod. The double connection setup of the pull-bending test allowed that the ERS gauges could be staggered left and right to minimise interference with the glueline. Similarly, where DTGs were used the rod was sanded along the entire length and the fibre was glued directly on to the rod using superglue. Previous research has shown that attaching the DTG fibres in this manner has no negative effect on readings obtained.

2.5 Test procedure

Samples were loaded in 0.5kN increments to failure using a UKAS calibrated 600kN capacity hydraulic actuator. Deflection at mid-span and net horizontal movement of the bar as the sample was loaded and recorded with data acquisition connected to the transducer. Failure load was recorded when the sample could not take any additional load. The mode of failure was recorded also – percentage failure mode was then calculated for each bonded length. Each test

was repeated nine times due to the high variability of the timber used.

3 EXPERIMENTAL RESULTS

3.1 Failure mode

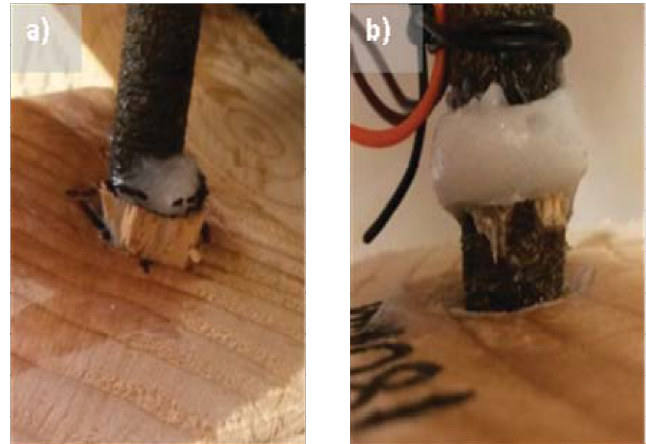


Figure 3. Failure modes observed: a) shear in timber, b) rod/adhesive failure

All specimens failed in a sudden, brittle manner. Two primary failure modes were identified and are pictured in Figure 3: a timber plug pull-out indicative of shear failure in the timber and a ‘clean’ pull-out signifying a failure of the rod/adhesive interface. In no cases was there failure within the adhesive or any rod failure.

The most prevalent failure mode observed was a pull-out failure in shear of the timber with a total of 67.6% of all samples failing in this manner. This was as expected due to the timber being the weakest element in the connection. Rod/adhesive failure was thought to have occurred due to the sand coating on the BFRP rod not adhering sufficiently well to the adhesive. The BFRP rod never failed since the force required for the rupture of the rod was never reached.

3.2 Suitability of test method

Strain data obtained from both methods of acquisition was reviewed and the most appropriate data set for each variable was chosen. It was established that for the majority of specimens using the ERS method proved to give the best data in terms of completeness.

With the shortest embedded length of $l_b=80\text{mm}$ using ERS gauges stress distribution was irregular at all load points. On inspection after failure it was observed that the adhesive had not formed a sufficient bond. It is suspected that this was due to the relatively large volume of wires prohibiting the formation of a good bond along the short embedded length. This was not a problem experienced with any of the larger embedded lengths.

A significant disadvantage highlighted with the use of the DTG fibre optic sensors was their fragility. In this case, on one of the specimens one sensor at the end of the fibre was damaged in the gluing process, leaving the data set incomplete.

3.3 Stress distribution along glued length

Generally, a linear increase in strain was observed at each measured location along the glued length until failure. In all specimens, the loaded end (0mm) recorded the maximum strain, proving the presumption that failure occurs primarily at the loaded end.

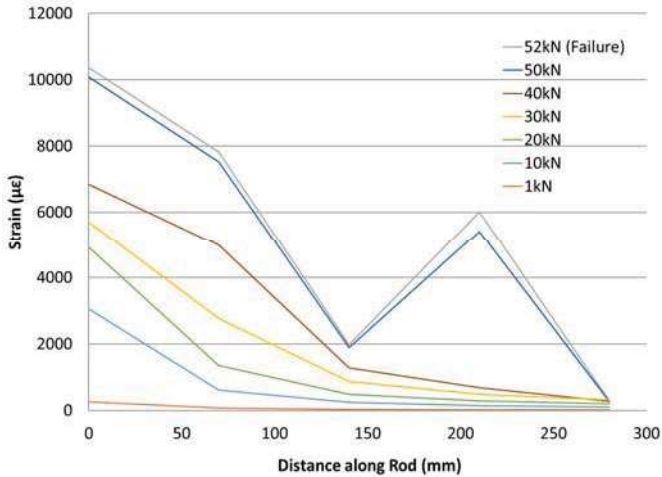


Figure 4. Stress distribution along glued length with increasing load ($l_b=280\text{mm}$, $a=42\text{mm}$)

Figure 4 illustrates the influence of increasing load on the stress distribution along the glued length. In a typical specimen stresses were distributed in a triangular fashion with the start of the glued length having the highest stress concentration and this dissipating along the glued length to a minimum concentration at the unloaded end. Further along the glued length it was observed that behaviour became more linear. This suggests that bending has less of influence on performance of the GiR further along the glued length than at the loaded end. As loading increased stresses increased at each measured location along the rod.

3.3.1 Influence of increasing edge distance, a

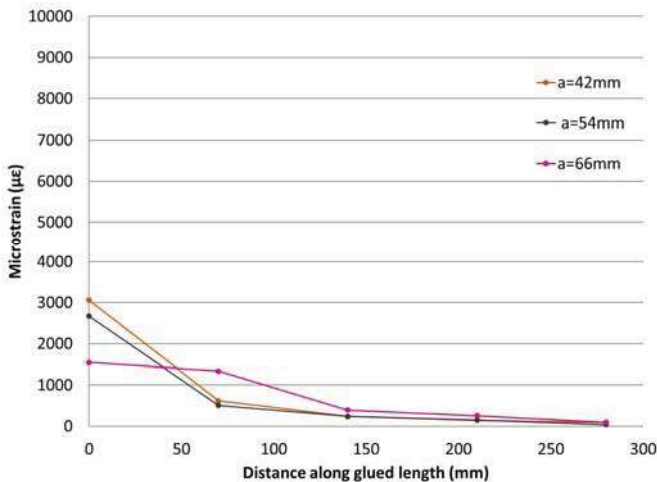


Figure 5. Stress distribution along glued length with increasing edge distance at a load of 10kN

Increasing edge distance tended to result in a reduction of stresses at each measured point along the bond length, as illustrated in Figure 5. When edge distance is increased the lever arm is reduced and hence the moment generated at the loaded end (0mm along rod) decreases.

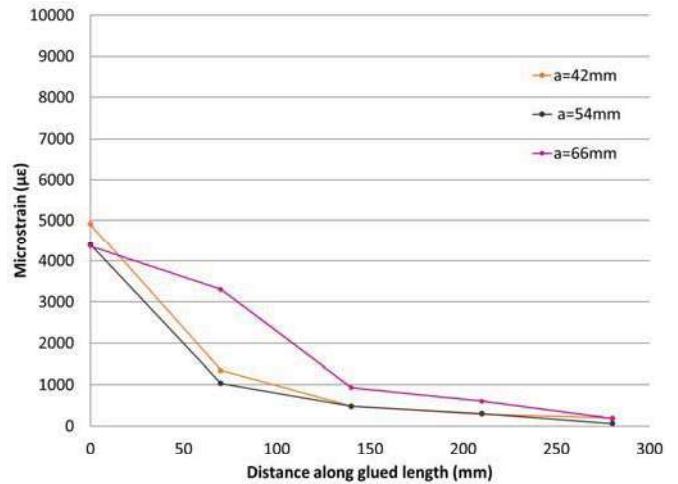


Figure 6. Stress distribution along glued length with increasing edge distance at a load of 20kN

With an increase in applied load the stress profile along the remained similar with an increase in stresses being observed at each measured location. Specimens with $a = 42\text{mm}$ and $a = 54\text{mm}$ failed at a similar ultimate load and both failed with a shear pull-out of the timber surrounding the bond. Specimen $a = 66\text{mm}$ failed at a lower load than the other two specimens and failure mode could not be visibly identified.

3.3.2 Influence of increasing embedded length, l_b

Increasing embedded length resulted in higher stresses being recorded at each measured location along the rod. Increased strain at the loaded end was observed with increasing embedded length. This is perhaps a result of a release of strain occurring in the shorter embedded lengths as the rod slips due to less anchorage in these specimens. However additional data must be collected to confirm this theory.

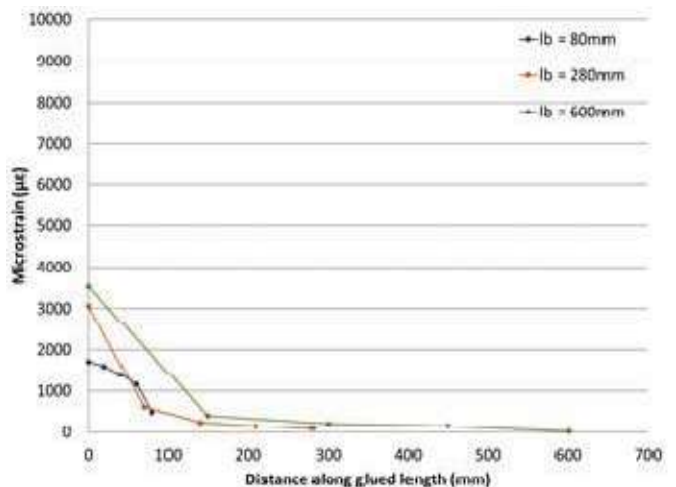


Figure 7. Stress distribution along glued length with increasing embedded length at a load of 10kN

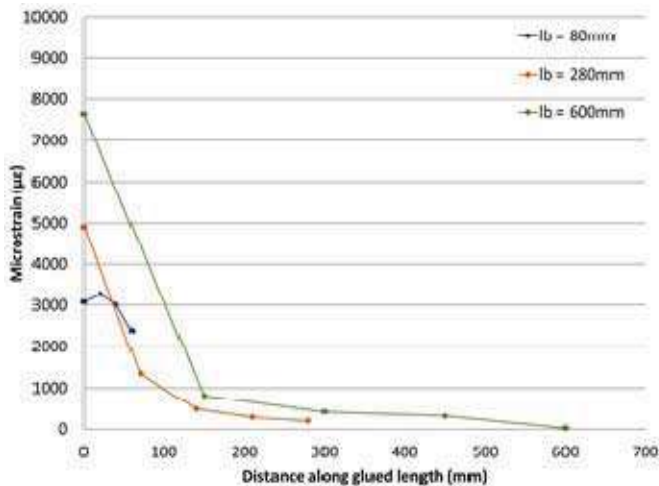


Figure 8. Stress distribution along glued length with increasing embedded length at a load of 20kN

As load increased, the distribution of stresses along the embedded length increased somewhat linearly, as seen in Figure 8. At a load of 20kN the shortest embedded length of $l_b = 80\text{mm}$ was nearing failure. With the sensors on this specimen spaced closer together than those on the other specimens an unzipping effect can be seen where failure propagates from the loaded end along the glued length. This is illustrated in Figure 8. It is not clear whether the other specimens evidenced this same movement of failure since the spacing between the first and second sensor on the glued length was considerably larger.

Although stresses did not increase as significantly at measured locations towards the anchored end than at the unloaded end it can be seen in Figure 7 and Figure 8 that there were some amount of stresses being carried towards the anchored end. This contradicts the findings of other researchers such as Yeboah [13] who suggested that the rod becomes inactive beyond an embedded length of 250mm and that no increase in strength is achievable beyond this length. As was observed in previous research by the authors, summarised in Section 2.1, the pull-out strength of the glued-in rods in this study continued to increase with increasing embedded length. This ability of the rod to carry stresses along the entire glued length explains how this increase in capacity is achieved. It is worth noting however that as the embedded length increases the stress capacity appears to be increasing at a lesser rate suggesting that a plateau in strength will be reached at some point.

4 CONCLUSIONS

- Experimental tests showed that the entire glued length of the glued-in rod connections contribute to resistance of the applied load, even in the longest embedded lengths.
- Stress distribution along the length of a glued-in rod under combined axial and bending force is not linear, with the loaded end reaching failure first and this then propagating along the glued length of the rod.

- Further work is suggested to assess the performance of such a connection method as a moment connection in a portal frame application.
- Higher loaded-end strains were observed for longer embedded lengths, further research should be undertaken to assess the slip behaviour with increasing embedded length.

ACKNOWLEDGMENTS

This research is funded by the Department of Agriculture, Food and the Marine of the Republic of Ireland under the FIRM/RSF/COFORD scheme as part of ‘Innovation in Irish timber Usage’ (project ref. 11/C/207). The authors would also like to thank the technical staff in QUB for their assistance in the lab.

REFERENCES

- [1] D. Smedley, P. Alam, and M. Ansell, “George Street, St. Albans, UK—a case study in the repair of historic timber structures using bonded-in pultruded plates,” ... *9th World Conf. Timber ...*, no. 2006, 2006.
- [2] K. U. Schober and K. Rautenstrauch, “Experimental Investigations on Flexural Strengthening of Timber Structures with CFRP,” in *Proceedings of the International Symposium on Bond Behaviour of FRP in Structures (BBFS 2005)*, 2005, pp. 457–464.
- [3] E. Gehri, “High Performing Jointing Technique Using Glued-in Rods,” in *11th World Conference on Timber Engineering 2010, WCTE 2010.*, 2010.
- [4] R. Bainbridge, C. Mettem, K. Harvey, and M. Ansell, “Bonded-in rod connections for timber structures—development of design methods and test observations,” *Int. J. Adhes. Adhes.*, vol. 22, no. 1, pp. 47–59, 2002.
- [5] J. G. Broughton and A. R. Hutchinson, “LICONS Task 2-Sub task 2.2,” 2004.
- [6] K. Harvey and M. P. Ansell, “Improved timber connections using bonded-in GFRP rods,” in *Proceedings of 6th World Conference on Timber Engineering, Whistler, British Columbia*, 2000.
- [7] M. Madhoushi and M. P. Ansell, “Experimental study of static and fatigue strengths of pultruded GFRP rods bonded into LVL and glulam,” *Int. J. Adhes. Adhes.*, vol. 24, no. 4, pp. 319–325, Aug. 2004.
- [8] M. Ansell and D. Smedley, “Briefing: Bonded-in technology for structural timber,” *Proc. ICE-Construction ...*, vol. 160, no. 3, pp. 95–98, Jan. 2007.
- [9] L. F. P. . F. P. Juvandes and R. M. T. Barbosa, “Bond Analysis of Timber Structures Strengthened with FRP Systems,” *Strain*, vol. 48, no. 2, pp. 124–135, 2012.
- [10] D. Yeboah, S. Taylor, D. McPolin, R. Gilfillan, and S. Gilbert, “Behaviour of joints with bonded-in steel bars loaded parallel to the grain of timber elements,” *Constr. Build. Mater.*, vol. 25, no. 5, pp. 2312–2317, 2011.
- [11] R. Steiger, E. Gehri, and R. Widmann, “Pull-out strength of axially loaded steel rods bonded in glulam parallel to the grain,” *Mater. Struct.*, vol. Vol. 40, no. 8, p. p 69–78, Jan. 2006.
- [12] M. Jahreis, K.-U. Schober, W. Haedicke, and K. Rautenstrauch, “Non-destructive testing , measurement and numerical damage analysis of high demanding stress regions in FRP reinforced timber structures by,” in *Composites 2010 American Composites Manufacturers Association*, 2010, pp. 1–6.
- [13] D. Yeboah, “Rigid Connections in Structural Timber Assemblies,” Queen’s University Belfast, 2012.
- [14] G. Tharmarajah, “Compressive Membrane Action in Fibre Reinforced Polymer (FRP) Reinforced Concrete Slabs,” Queen’s University Belfast, 2010.
- [15] E. Serrano, “Glued-in rods for timber structures * a 3D model and nite element parameter studies,” vol. 21, pp. 115–127, 2001.
- [16] J. G. Broughton and A. R. Hutchinson, “Adhesive systems for structural connections in timber,” *Int. J. Adhes. Adhes.*, vol. 21, no. 3, pp. 177–186, 2001.
- [17] Rotafix Ltd, “Rotafix Structural Adhesive (LM) - Epoxy Bonding Adhesive,” 2015.